A245 : Optical Frequency Doubling

A lab report written by

Group P20: Mrunmoy Jena and Ajay Shanmuga Sakthivasan

Supervisor: Thilina Muthu-Arachchige

Contents

Abstract

xyz

Introduction

Experiment and Analysis of Results

This section discusses the experimental setup and procedure, along with the calculation of the necessary quantities and their error analysis.

To begin with, a class 3B external cavity diode laser (TuiOptics, DL100) which was set to emit light of wavelength 987 nm, was used for the experiment. A shutter mounted onto the laser controlled the beam and a pair of anamorphotic prisms was used to modify the elliptical beam profile to a more circular shape. The laser, shutter and prism pairs were all fixed on an optical table beforehand. For each part of the experiment, other instruments and optical elements were added onto this set-up.

2.1 Power measurements of the diode laser

The first part of the experiment is aimed at familiarizing oneself with the dependence of the fundamental output power of the laser with the injection current and to extract various important parameters characterizing the laser such as the threshold current, differential slope efficiency and the differential quantum efficiency.

In order to perform this experiment, a power meter was mounted on table in such a manner that it remained at the same height as that of laser beam as well as aligned with the beam (i.e. the face of the power meter was perpendicular to the beam axis). This adjustment was first performed by using an IR (infrared) detection card in order to ensure that the entire beam went into the power meter. Then the power meter was switched on, and the wavelength to be measured by it was set to 987 nm. Subsequently, finer adjustment was performed by moving the power meter to a position where it gave the maximum power reading. The power meter was then screwed tight at this position.
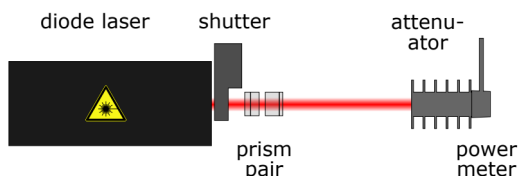

Figure 2.1: Set up to measure variation of laser output power with injection current [1]

The set up for this experiment (along with attenuator attached) is shown in Figure 2.1. With this setup in place, the injection current was increased from 0 to 280 mA in increments of 5 mA, and the corresponding values of output power were noted. Since the power meter sensor becomes non-linear for powers above 20 mW, it becomes necessary to use an attenuator. For our measurements, we took measurements both with, and without attenuator in the unattenuated power range from 28.2 μW to 19000 μW (19 mW). Both the unattenuated and attenuated power values are essential to be recorded over at least some data points in order to perform the calibration and extract a calibration factor from it. Beyond this range, the power was only measured with the attenuator attached onto the power meter, due to the aforementioned reason of non-linearity of the sensor. The attenuator for the experiment was

a '1000:1' attenuator (meaning that ideally it reduces the unattenuated power by a factor of 1000). The recorded data can be found in A.1. The values measured without attenuator are listed under the column 'P_{unatt}' and the measured power values with attenuator are under the column 'P_{att}'. From now on, all errors stated in the tables should be assumed to be instrumental errors (least count of the measuring instrument), unless otherwise stated.

2.1.1 Calibration of removable attenuator

In order to find the calibration factor, the data for the attenuated power vs. unattenuated power is plotted and a linear fit is applied to this dataset. To carry out the curve fitting procedure using the data points and some initial guess parameters, we used the function `curve_fit()` from the `scipy.optimize` module for *Python*. The data points (along with x-y error bars) and the linear fit modelled onto them is shown in Figure 2.2.
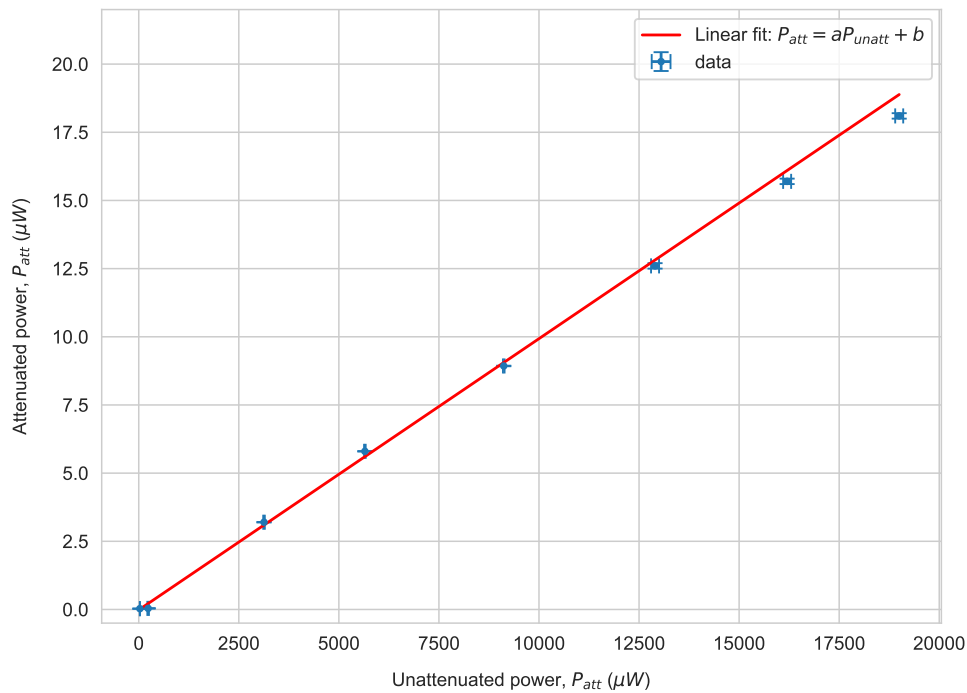
Figure 2.2: Calibration plot of attenuated output power vs unattenuated power

The linear fit chosen is of the form:

$$P_{att} = aP_{unatt} + b \tag{2.1}$$

The choice of the initial guess parameters is taken as $a = 0.001$ (since as already mentioned before, attenuated power is around 1/1000 of the unattenuated power, due to use of '1000:1' attenuator) and $b = 0$ (y intercept expected to be a very small value, by visually extrapolating the data points). Indeed, after running the curve fitting procedure, we get fit parameters close to our initial guess: $a = 0.000994\pm$

1.25×10^{-6} and $b = -0.016 \pm 0.006$, giving:

$$P_{att} = (0.000994 \pm 1.25 \times 10^{-6})P_{unatt} + (-0.016 \pm 0.006)$$

Now we use the commonly applied reduced χ^2 test, to find the goodness of fit for this linear model:

$$\chi^2 = \sum_i \left[\frac{y_i(x_i) - f_i(x_i; p)}{\sigma_i} \right]^2 \tag{2.2}$$

where $y_i(x_i)$ are the recorded y values (attenuated power in this case), $f_i(x_i; p)$ is are y values from the fitting function with p parameters (in this case the linear fit function with parameters a and b).

Surprisingly, we get an extremely large reduced χ^2 value of 174.69. Naively, one would conclude that since $\chi^2 \gg 1$, the model is a 'bad fit'. However, on looking more carefully at the data points, we make two observations:

- We find that the error in the first five data points (corresponding to current (I) values lying in the range of 50 to 70 mA) is an order of magnitude smaller than for the remaining data points. Given that the order $\mathcal{O}(y_i(x_i) - f_i(x_i; p))$ remains the same (more or less), the χ^2 is sensitive to the order of the squares of the y-errors $\mathcal{O}(\chi^2) \sim \mathcal{O}\left(1/\sigma_i^2\right)$. As such, the contribution from the very small errors of the first five data values would be around 100 times compared to that from the remaining y values.

- Moreover, we only have a small number of data points ($N = 8$), which we are trying to fit with two parameters ($p = 2$), this restricts the degrees of freedom to only 6 ($df = N - p$). Again this leads to a large reduced χ^2 value.

The combination of both these factors shows that in the case of small data sets, the error on the data points largely affects the reduced χ^2 value. Indeed, this is confirmed in a paper by Andrae et.al. [2]. However, here, since we are concerned with only extracting the calibration factor, we just want to check how well the linear regression line approximates the actual data values. For this we calculate the R^2 (coefficient of determination):

$$R^2 = 1 - \frac{\sum_i \left(y_i - f_i(x_i; p)\right)^2}{\sum_i \left(y_i - \bar{y}\right)^2} \tag{2.3}$$

where $\bar{y}$ is the mean of all the recorded data values

The R^2 value indeed comes out to be very close to 1 ($R^2 = 0.997$), meaning that our linear model explains 99.7% of all the variation of the y value (attenuated power) around its mean.

2.1.2 Calculation of unattenuated power values above 19 μW

We recall that after the unattenuated power reached a value of 19 μW, only attenuated power values were recorded. Therefore, in order to find the dependence of unattenuated power with the injection current, we need to use to calculate unattenuated power values above 19 μW first, by applying the calibration factor to the attenuated power values. From Eq. 2.1 we get:

$$P_{unatt} = \frac{P_{att} - b}{a} \tag{2.4}$$

In addition to this, the errors on each of these calculated values will no longer be instrumental, but will be calculated from error propagation:

$$\Delta P_{unatt} = \sqrt{\left(\frac{\Delta P_{att}}{a}\right)^2 + \left(\frac{\Delta b}{a}\right)^2 + \left(\frac{\Delta a(P_{att} - b)}{a^2}\right)^2} \tag{2.5}$$

These calculated unattenuated power values and their errors are also included in Table A.1.

2.1.3 Study of dependence of fundamental output power on the injection current

Once all the unattenuated power values are obtained, the fundamental unattenuated power vs injection current is plotted. This plot is shown in Figure 2.3.
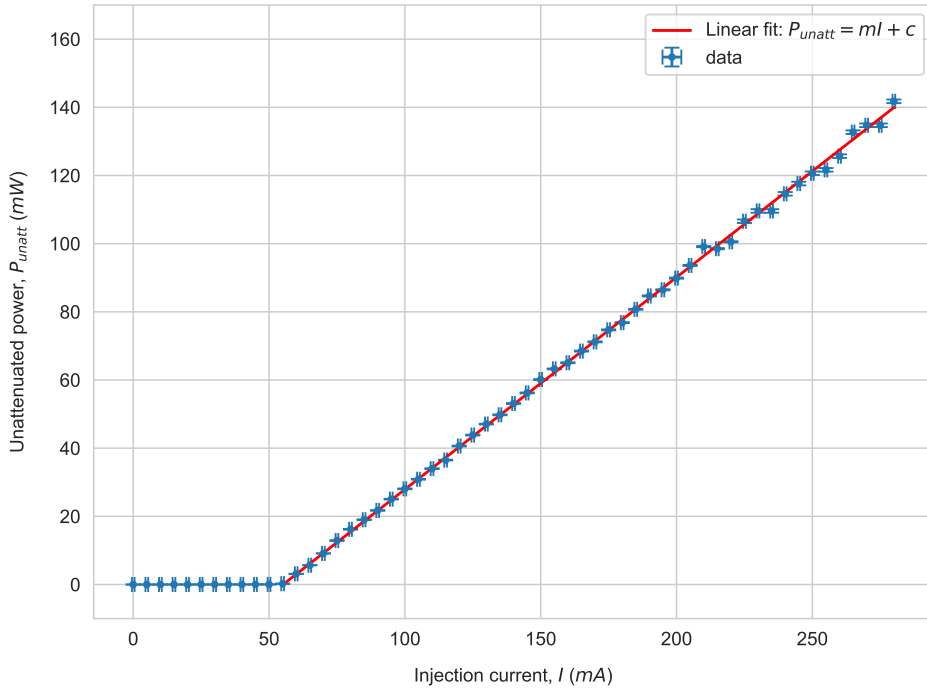
Figure 2.3: Plot of unattenuated output power vs injection current

One finds that the unattenuated power remains close to zero upto a certain value of the injection current (around 50 mA) and after this value, the fundamental power starts increasing linearly with the injection current. As such, for this linear region, we choose a linear fit of the form:

$$P_{unatt} = mI + c \tag{2.6}$$

After visually guessing the slope and the y intercept, we take initial parameters for curve fitting as $m = 30/40 = 0.75$ and $c = -30$. The least square curve fitting procedure gives the best linear fit

as:

$$P_{unatt} = (0.62234 \pm 0.00027)I + (-34.329 \pm 0.022) \text{ mW} \tag{2.7}$$

The R^2 value for this fit is found to be 0.9993, indicating a linear model that explains the variability in y values quite well. Again, the χ^2 goodness of fit test isn't used here because of the complications mentioned in Section 2.1.1.

2.1.4 Calculation of laser output characteristics

- **Threshold current:** The particular value of injection current, at which the output unattenuated power starts increasing from zero is called the threshold current and is given by:

$$I_0 = -\frac{c}{m} \tag{2.8}$$

while its error is found to be:

$$\Delta I_0 = \sqrt{\left(\frac{\Delta c}{m}\right)^2 + \left(\frac{c\Delta m}{m}\right)^2} \tag{2.9}$$

This gives a threshold current value of $I_0 = 55.161 \pm 0.039$ mA

- **Differential slope efficiency:** The differential slope efficiency, in the case of this linear fit is simply the slope of the straight line:

$$\frac{\partial P}{\partial I} = \frac{P}{I} = m \tag{2.10}$$

with its error given as:

$$\Delta\left(\frac{\partial P}{\partial I}\right) = \Delta m \tag{2.11}$$

The result is then $\frac{\partial P}{\partial I} = -34.329 \pm 0.022$ W/A

- **Quantum efficiency:** The quantum efficiency is given by the ratio of the number of photons that are emitted (N_γ) to the number of injected electrons (N_e). This is then given as:

$$\eta = \frac{N_\gamma}{N_e} = \frac{e}{h\nu}\frac{\partial P}{\partial I} \tag{2.12}$$

with error:

$$\Delta\eta = \frac{N_\gamma}{N_e} = \left(\frac{e}{h\nu}\right)\Delta\left(\frac{\partial P}{\partial I}\right) = \left(\frac{e\lambda}{hc}\right)\Delta\left(\frac{\partial P}{\partial I}\right) \tag{2.13}$$

where e is the fundamental unit of electric charge, h is Planck's constant and ν is the frequency of light given as c/λ. The quantum efficiency is then found to be $\eta = 0.495 \pm 0.00021$. The interpretation of this value is that on an average, for every 2 ($\sim 1/\eta$) electrons injected into the laser diode, 1 photon was emitted.

2.1.5 Calibration of variable attenuator

We observed that controlling the laser fundamental power by varying the diode current is an inefficient method since the power of the laser did not vary continuously with the injection current. Instead jumps in power and frequency occurred when we did this (known as 'mode hops') [1]. Therefore the previous setup was modified by introducing a rotatable $\lambda/2$ plate and a beam splitter cube (both of which function as two polarizers), in the beam path between the laser diode and the power meter. The injection current

was fixed at its maximum value for this part of the experiment. First, we checked that the beam splitter cube was placed such that it transmitted the maximum possible power without the $\lambda/2$ plate. After this was ensured, the $\lambda/2$ plate was inserted. Moreover, as done before, in order to precisely adjust the heights and positions of the optical elements, an IR card was used to follow the beam path and ensure that the entire transmitted beam falls completely on the power meter. The schematic set up for this part of the experiment is shown in Figure 2.4.
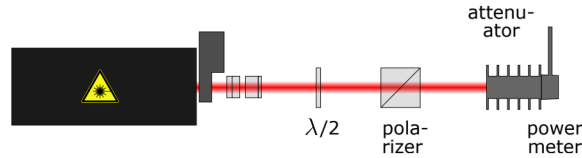
Figure 2.4: Schematic set up for variable attenuator calibration [1]

Now, in order to find the dependence of transmitted fundamental power with the angle of polarization, we rotated the $\lambda/2$ plate in a clockwise direction, starting from 0° upto 180° in increments of 2.5°. A non linear, $\cos^2\theta$ form of fitting curve is chosen for this data, since we expect this variation to follow Malus' law. Both the plot of this variation along with the fitting curve are displayed in Figure 2.5.
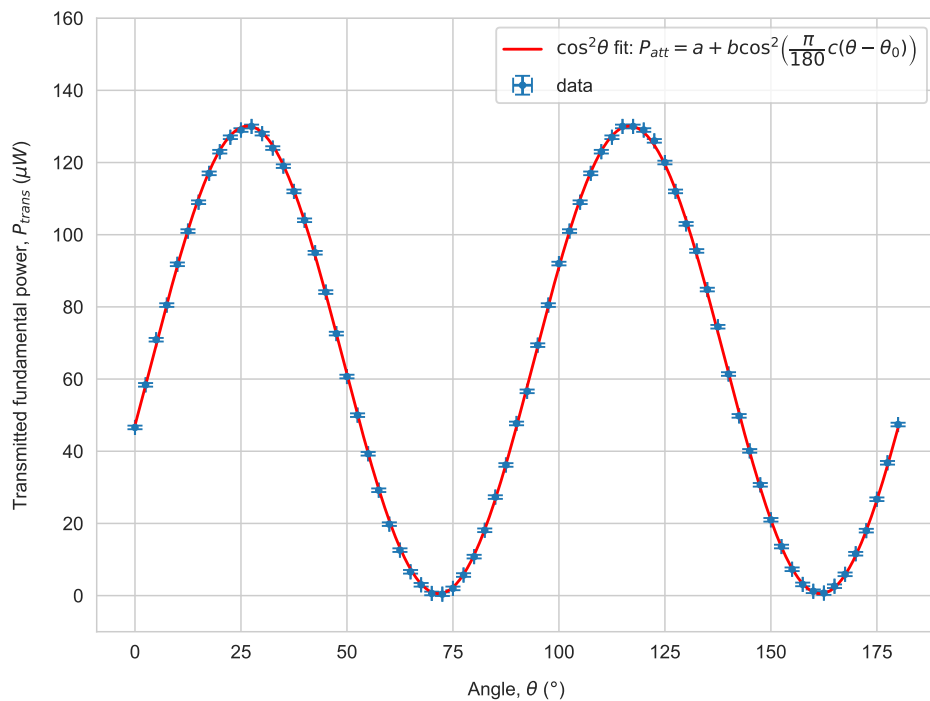
Figure 2.5: Plot of the transmitted fundamental power vs the rotation angle of the $\lambda/2$ plate

The exact form of the fitting function is taken as follows:

$$P_{trans} = a + b\cos^2\left(\frac{\pi}{180}c(\theta - \theta_0)\right) \tag{2.14}$$

where the parameter a represents the minimum transmitted power, b represents the difference between the maximum and minimum transmitted power, c being the factor by which the beam was rotated by the $\lambda/2$ plate and θ_0 representing the angle of $\lambda/2$ plate at which maximum power was measured. The factor of $\pi/180$ is simply there to convert the measured angles in degrees to radians since the cosine function, `numpy.cos()` used in *Python* accepts angles in radians. By visually inspecting the plots of the data points, the initial guess parameters for the fitting function are taken as: $a = 0$, $b = 130$, $c = 2$ (expected to be 2 since a rotation of the $\lambda/2$ plate by θ would rotate plane of polarization of the initial beam by 2θ), $\theta_0 = 0$. After fitting, the optimal parameters come out to be:

$$a = (0.540 \pm 0.102) \ \mu W$$
$$b = (129.561 \pm 0.167) \ \mu W$$
$$c = 1.9983 \pm 0.0007$$
$$\theta_0 = (26.590 \pm 0.027)°$$

Therefore the fitting function becomes:

$$P_{trans} = (0.540 \pm 0.102) + (129.561 \pm 0.167)\cos^2\left(\frac{\pi}{180}(1.9983 \pm 0.0007)(\theta - (26.590 \pm 0.027))\right) \ \mu W \tag{2.15}$$

As the data in this case is free from the complications discussed in Section 2.1.1, we use the χ^2 test for goodness of fit. The reduced χ^2 value comes out to be 1.47, which tells us that that the model $\cos^2\theta$ curve fits the data (including the respective errors) well enough.

Given that we now have a calibration curve that describes the variation of transmitted fundamental power with the polarization angle, it is possible to measure just the variation of second harmonic power with the angle, θ to in turn get the dependence of second harmonic power on fundamental power, using the calibration curve.

Additionally, we calculate the extinction ratio, which is defined as the ratio of the maximum transmitted power to minimum transmitted power:

$$\eta_{ext} = \frac{P_{max}}{P_{min}} = \frac{a+b}{a} \tag{2.16}$$

with its error as:

$$\Delta\eta_{ext} = \sqrt{\left(\frac{\Delta b}{a}\right)^2 + \left(\frac{b\Delta a}{a^2}\right)^2} \tag{2.17}$$

This gives us an extinction ratio of $\eta_{ext} = 240.683 \pm 45.024$

2.2 Second harmonic wave generation

In this part of the experiment, the laser beam is directed into the non-linear crystal ($KbNO_3$, potassium niobate) and variations of the second harmonic power with different parameters (such as the crystal

temperature, fundamental wave power and angle of polarization of fundamental wave) is recorded.

2.2.1 Focusing the laser beam into the non-linear crystal

The first step for second harmonic wave generation was to devise a method to focus the laser beam into the crystal and subsequently collimate the light transmitted through the crystal. The diagram of the entire set up is displayed in Figure 2.6
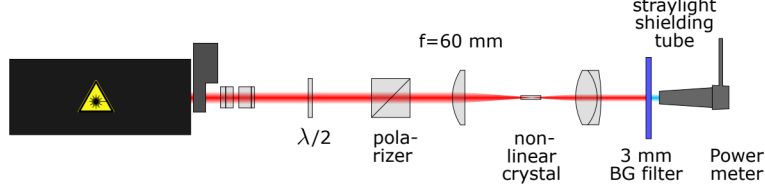

Figure 2.6: Configuration for focusing of fundamental wave and subsequent collimation of light transmitted through the non-linear crystal [1]

The focusing lens was necessary to ensure that the entire intensity of the incident beam entered the non-linear crystal, which would then mean that a second harmonic beam having the maximum possible power/intensity would be generated. In order to accomplish this, we used a plano-convex lens with a focal length of $f = 60$ mm. The lens was placed such that its convex surface faced the incoming beam and the plane surface faced the opposite direction. We noted that in order for the incident beam to be maximally focused when it enters the crystal, the distance between the focusing lens and the crystal needs to a equal to the focal length (60 mm) of the lens. This distance was measured with a scale and the position where the lens would then be placed is marked. However, before placing the lens, we needed to ensure that the beam fell exactly on the center of the focusing lens. To do this, we used a screen (which in this case was an upright stand with paper taped onto it) and placed it at some distance further from where the lens was to be placed. With the help of an IR card, the size of the laser beam spot was marked on the screen. Now, the focusing lens was placed at the decided position and finer adjustment of its position was done so that the beam falling on the screen now had a spot that exactly overlapped the one marked before placing it. Another consideration was that the lens surface had to perpendicular to the beam path, i.e the optical axis of the lens needed to be aligned with the beam path. This was important because deviation of the optic axis from the beam path would produce undesirable effects such as coma and astigmatism [1]. To do this we first checked if the beam path was itself parallel to the surface of the optical table as well as to the rows of holes on it. Then, it was visually ensured that the lens surface was perpendicular to the table and to the incoming beam axis. The rows of holes on table again assisted us in doing this. Finally, the lens was clamped at the optimal position.

Now, the fundamental beam was transmitted through the crystal and using the IR card, it could be seen on the other side. However, this beam was slightly diverging and in order to get the maximum power measurement at the power meter, we needed to use a collimating lens. The lens used for this purpose was again a plano-convex lens (having a focal length of 30 mm), with its convex surface now facing the incoming beam. As done before, this lens was placed at distance equal to its focal length, away from the crystal. Again, it was visually ensured that the lens was upright (perpendicular to the table) and also perpendicular to the beam path. Finer adjustment of the lens position (along beam axis) was

made by moving the screen over an appreciable distance along the (supposedly) collimated beam path and observing if the beam spot size remains the same (with the help of the IR card). After all these adjustments, the collimating lens position was finalized and it was clamped to the optical table.

2.2.2 Optimizing the second harmonic power

In order for us to clearly observe the second harmonic wave generated by the crystal, we needed to bring the crystal to a temperature where it gives maximum intensity of second harmonic light. For the case of the $KbNO_3$ crystal, it is found to be around 36.7 °C [1]. Therefore, in the present experiment, the crystal was slowly heated up from 27 °C to 36.7 °C in small increments of 0.5 °C. Once this peak temperature was reached, with the crystal properly aligned with the beam direction, we could clearly see a blue light spot on the screen placed after the lens (along the direction of beam propagation), indicating that the SH (second harmonic) light had been generated.

The crystal arrangement had been mounted onto a stand that had threaded screws for finer adjustment of crystal position in all three directions. In order to perfectly optimize the intensity of SH light generated, the power meter was turned on, its wavelength setting was set to 493.5 nm (half of the fundamental wavelength) and the power reading was noted. Using the threaded screws on the aforementioned arrangement, the crystal position was fine tuned, so that a maximum value of power was measured. While fine tuning, it was noticed that the SH power goes down significantly if the fundamental beam falls on to the edges to the crystal (since it will then not be entirely converted to SH light), therefore crystal position was adjusted so that the beam was incident at the center of the crystal. The generation of the SH blue light illuminated the crystal edges clearly, which made it easy for us to do this adjustment. Since only the SH power was to be recorded, a BG40 glass filter, of thickness 3 mm was used to block out the infrared fundamental wave component. Further, in order to prevent any background signal from affecting the actual SH reading, we mounted a conical stray-light shielding tube onto the measuring surface of the power meter. All readings that would be subsequently be reported in this section, had been recorded with the stray-light shielding tube attached.

On optimization, the SH beam power was found to have a maximum value of 36.6 μW which is slightly lower than the desirable optimal value of 40 μW [1]. This can be attributed to the fact that the theoretical value of 36.7 °C might not exactly be the temperature at which the SH intensity is maximum. This temperature was later on adjusted more precisely while studying dependence of SH power on crystal temperature.

2.2.3 Calculation of Gaussian beam parameters

The next step would be to check how close the parameters of the generated SH beam are to the optimal values of Gaussian beam parameters. To this end, we first list out some pre-calculated parameters and constants given in lab instruction manual [1]. (Note: values of focal length, refractive index, length of crystal and wavelength have been stated without any associated errors in the manual, and therefore they have been taken as such).

- Crystal refractive index, $n = 2.2$

- Fundamental beam wavelength, $\lambda = 987$ nm

- Focal length of focusing lens, $f = 60$ mm

- Length of non-linear crystal, $L = 5$ mm

- Beam diameter before entering lens, $d = (3.5 \pm 0.5)$ mm

Now, we calculate the beam parameters:

- **Beam waist:** The beam waist is given by:

$$\omega_0 = \frac{2f\lambda}{\pi d} \tag{2.18}$$

  and its error is calculated as:

$$\Delta\omega_0 = \frac{2f\lambda}{\pi}\left(\frac{\Delta d}{d}\right) \tag{2.19}$$

  This gives us a value of $\omega_0 = 10.771 \pm 5.386$ μm

- **Rayleigh length:** The Rayleigh length is defined as:

$$z_0 = \frac{\pi n \omega_0^2}{\lambda} \tag{2.20}$$

  and has an error:

$$\Delta z_0 = \frac{2\pi n \omega_0 \Delta\omega_0}{\lambda} \tag{2.21}$$

  We get the value of Rayleigh length as $z_0 = 0.812 \pm 0.406$ mm

- **Confocal parameter:** The confocal parameter is given as:

$$b = 2z_0 \tag{2.22}$$

  with an error:

$$\Delta b = 2\Delta z_0 \tag{2.23}$$

  This gives a value of $b = 1.625 \pm 0.812$ mm

- **Boyd Kleinman condition:** For maximal efficiency of SH wave power generation, one needs to have the crystal length (L) and confocal parameter (b) in the ratio:

$$\frac{L}{b} = 2.84 \tag{2.24}$$

  with the error calculated as:

$$\Delta\left(\frac{L}{b}\right) = \frac{L\Delta b}{b^2} \tag{2.25}$$

  Putting in the values of L and b in our case, we get the ratio as: $L/b = 3.077 \pm 1.538$. We see that this value for our set up is close to the optimal value, within the calculated error bounds.

- **Optimal focal length:** The optimal focal length for this experiment can be calculated by using the obtained Boyd-Kleinman ratio and substituting the expression for b in terms of focal length (f), and then solving the equation:

$$\frac{L}{b} = \frac{L}{2z_0} = \frac{\lambda L}{2\pi n \omega_0^2} = \frac{\pi d^2 L}{8nf^2\lambda} = 3.077$$

This gives us:

$$f_{opt} = \sqrt{\frac{\pi d^2 L}{24.616 n \lambda}} \tag{2.26}$$

with an error:

$$\Delta f_{opt} = \sqrt{\frac{\pi L}{24.616 n \lambda}} \Delta d \tag{2.27}$$

The value obtained for the optimal focal length is then $f_{opt} = 60.000 \pm 8.571$ mm. Clearly this matches with the focal length of the lens that we have used, although we find that there is a large theoretical uncertainty on it as calculated from the error propagation.

Bibliography

[1] Universität Bonn, *A245 experiment description.*

[2] R. Andrae, T. Schulze-Hartung, and P. Melchior, *Dos and don'ts of reduced chi-squared*, 2010.

Appendix

Table A.1: Measured unattenuated and attenuated power of the fundamental beam vs the injection current

I (mA)	ΔI (mA)	P_{unatt} (μW)	ΔP_{unatt} (μW)	P_{att} (μW)	ΔP_{att} (μW)
0	0.5	0	0.01	0	0
5	0.5	1.4	0.01	0	0
10	0.5	3	0.01	0	0
15	0.5	5.1	0.01	0	0
20	0.5	7.3	0.01	0	0
25	0.5	9.6	0.01	0	0
30	0.5	12.2	0.1	0	0
35	0.5	15.6	0.1	0	0
40	0.5	18.6	0.1	0	0
45	0.5	22.7	0.1	0	0
50	0.5	28.2	0.1	0.03	0.01
55	0.5	235	20	0.04	0.01
60	0.5	3130	20	3.2	0.01
65	0.5	5650	20	5.8	0.01
70	0.5	9120	20	8.93	0.01
75	0.5	12900	100	12.6	0.1
80	0.5	16200	100	15.7	0.1
85	0.5	19000	100	18.1	0.1
90	0.5	21730	104	21.6	0.1
95	0.5	25048	106	24.9	0.1
100	0.5	28064	107	27.9	0.1
105	0.5	30879	108	30.7	0.1
110	0.5	33995	109	33.8	0.1
115	0.5	36508	111	36.3	0.1
120	0.5	40630	113	40.4	0.1
125	0.5	43847	115	43.6	0.1
130	0.5	47064	117	46.8	0.1
135	0.5	49778	119	49.5	0.1
140	0.5	53095	121	52.8	0.1
145	0.5	56212	123	55.9	0.1
150	0.5	60132	126	59.8	0.1
155	0.5	63249	128	62.9	0.1
160	0.5	65058	130	64.7	0.1
165	0.5	68476	133	68.1	0.1
170	0.5	71190	135	70.8	0.1
175	0.5	74709	138	74.3	0.1
180	0.5	76820	140	76.4	0.1
185	0.5	80740	143	80.3	0.1
190	0.5	84661	147	84.2	0.1
195	0.5	86470	148	86	0.1
200	0.5	89888	152	89.4	0.1
205	0.5	93608	155	93.1	0.1
210	0.5	99137	160	98.6	0.1
215	0.5	98534	160	98	0.1
Continued on next page					

Table A.1 – continued from previous page

I (mA)	ΔI (mA)	P_{unatt} (μW)	ΔP_{unatt} (μW)	P_{att} (μW)	ΔP_{att} (μW)
220	0.5	100544	162	100	0.1
225	0.5	106576	520	106	0.5
230	0.5	109592	521	109	0.5
235	0.5	109592	521	109	0.5
240	0.5	114618	523	114	0.5
245	0.5	117634	524	117	0.5
250	0.5	120650	525	120	0.5
255	0.5	121655	526	121	0.5
260	0.5	125676	527	125	0.5
265	0.5	132713	530	132	0.5
270	0.5	134724	531	134	0.5
275	0.5	134724	531	134	0.5
280	0.5	141761	533	141	0.5

Table A.2: Attenuated fundamental beam power measured at different angles of rotation of $\lambda/2$ plate

θ (°)	$\Delta\theta$ (°)	P (μW)	ΔP (μW)	θ (°)	$\Delta\theta$ (°)	P (μW)	ΔP (μW)
0	0.5	46.6	0.5	92.5	1	56.6	0.5
2.5	1	58.4	0.5	95	0.5	69.4	0.5
5	0.5	70.9	0.5	97.5	1	80.5	0.5
7.5	1	80.5	0.5	100	0.5	92	0.5
10	0.5	91.8	0.5	102.5	1	101	0.5
12.5	1	101	0.5	105	0.5	109	0.5
15	0.5	109	0.5	107.5	1	117	0.5
17.5	1	117	0.5	110	0.5	123	0.5
20	0.5	123	0.5	112.5	1	127	0.5
22.5	1	127	0.5	115	0.5	130	0.5
25	0.5	129	0.5	117.5	1	130	0.5
27.5	1	130	0.5	120	0.5	129	0.5
30	0.5	128	0.5	122.5	1	126	0.5
32.5	1	124	0.5	125	0.5	120	0.5
35	0.5	119	0.5	127.5	1	112	0.5
37.5	1	112	0.5	130	0.5	103	0.5
40	0.5	104	0.5	132.5	1	95.5	0.5
42.5	1	95	0.5	135	0.5	84.8	0.5
45	0.5	84.1	0.5	137.5	1	74.5	0.5
47.5	1	72.6	0.5	140	0.5	61.4	0.5
50	0.5	60.7	0.5	142.5	1	49.8	0.5
52.5	1	50	0.5	145	0.5	40.1	0.5
55	0.5	39.3	0.5	147.5	1	30.7	0.5
57.5	1	29.2	0.5	150	0.5	21	0.5
60	0.5	19.8	0.5	152.5	1	13.6	0.5
62.5	1	12.6	0.5	155	0.5	7.3	0.5
65	0.5	6.6	0.5	157.5	1	3.1	0.5
67.5	1	3	0.5	160	0.5	1.2	0.5
70	0.5	0.6	0.5	162.5	1	0.7	0.5
72.5	1	0.4	0.5	165	0.5	2.6	0.5
75	0.5	2	0.5	167.5	1	5.9	0.5
77.5	1	5.7	0.5	170	0.5	11.6	0.5
80	0.5	10.8	0.5	172.5	1	18	0.5
82.5	1	18.1	0.5	175	0.5	26.7	0.5
85	0.5	27.3	0.5	177.5	1	36.8	0.5
87.5	1	36.2	0.5	180	0.5	47.4	0.5
90	0.5	47.7	0.5				